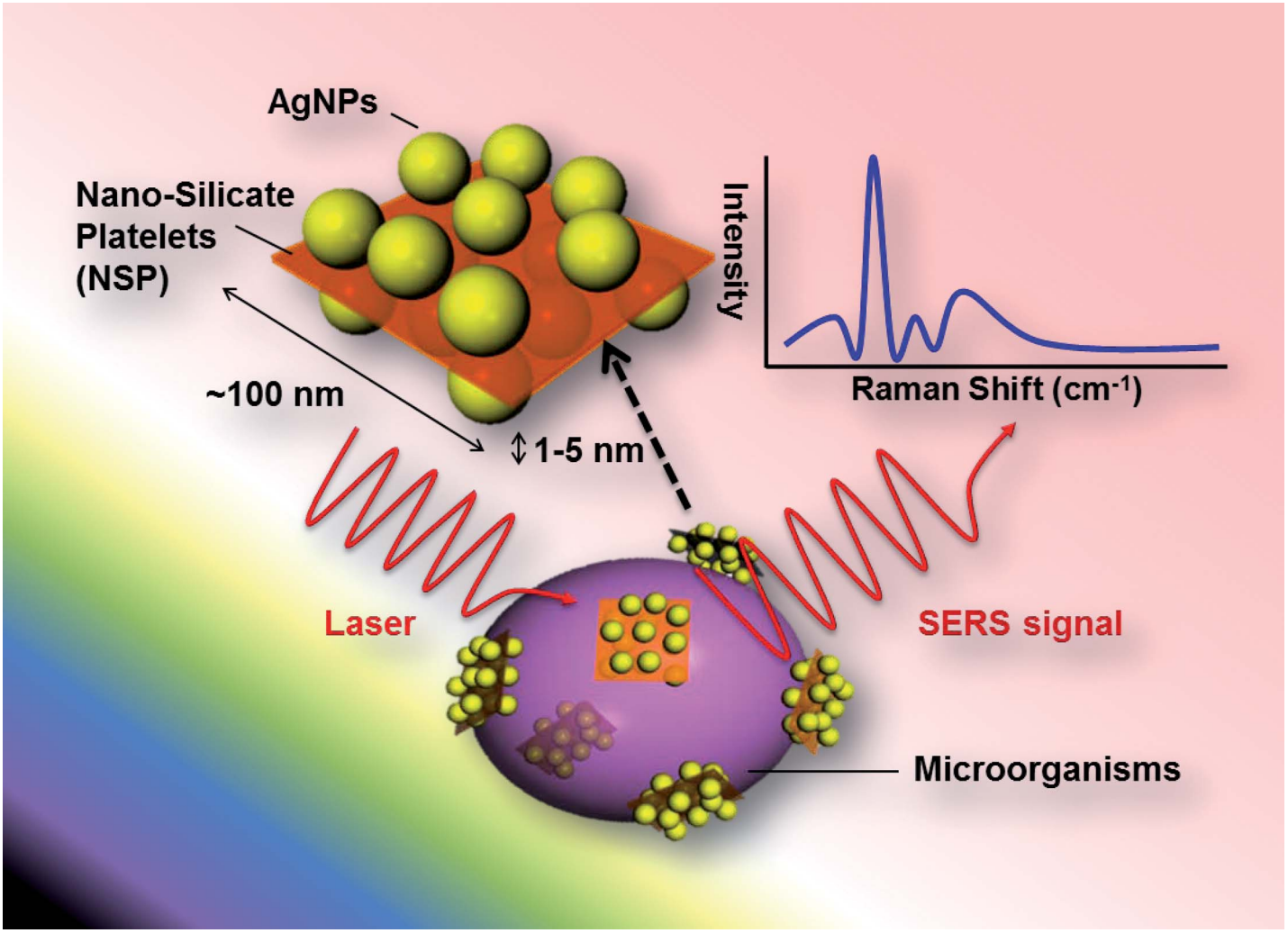

Showcasing research from Prof. T. Y. Liu's Lab at Ming Chi University of Technology and Prof. J. J. Lin's Polymer Lab at National Taiwan University, Taiwan.

Title: Label-free and culture-free microbe detection by three dimensional hot-junctions of flexible Raman-enhancing nanohybrid platelets

A novel flexible and 3D hot-junction SERS substrate of silver nanoparticles on nano-silicate platelets allows the detection of microbes with high efficiency.

As featured in:

See T. Liu *et al.*, *J. Mater. Chem. B*, 2014, **2**, 1136.

ROYAL SOCIETY OF CHEMISTRY

www.rsc.org/MaterialsB

Registered charity number: 207890

Journal of Materials Chemistry B

PAPER

Label-free and culture-free microbe detection by three dimensional hot-junctions of flexible Raman-enhancing nanohybrid platelets†

Cite this: *J. Mater. Chem. B*, 2014, **2**, 1136

Ting-Yu Liu,*[ab] Jun-Ying Ho,[a] Jiun-Chiou Wei,[a] Wei-Chih Cheng,[c] I.-Hui Chen,[de] Jessie Shiue,[de] Huai-Hsien Wang,[c] Juen-Kai Wang,[cf] Yuh-Lin Wang[cg] and Jiang-Jen Lin*[a]

Novel nanohybrid arrays of silver (Ag)-on-silicate platelets with flexibility and three-dimensional (3D) hot-junctions (particularly in *z*-direction) were discovered for improving the stability of free nanoparticles and the mobility of rigid (glass or silicon-based) substrates in surface-enhanced Raman scattering (SERS) detection technology. Since the Ag nanoparticles are adsorbed on both sides of few nanometer-thick silicate platelets (single-layer exfoliated clay), the geometric arrangement of Ag on both sides of the nanoplatelets (Ag/NSP) may induce strong hot-junctions (*z*-direction) in reference to the pristine montmorillonite clay (multi-layers) at the thickness of ~20 nm, measured by small molecules (adenine of DNA) and bacteria (*S. aureus*). Enormous red-shifts (16 nm wavelength difference) were observed between single layer and multi-layer silicate platelets, showing that huge surface plasmon enhancement comes from hot junctions in the *z*-direction (~7 times higher than 2D hot-junctions of traditional SERS biochips). Further, the Ag/NSP SERS substrate displays a free floating mobility and optical transparency (less background interference), which inherently increase the contacted surface-area between the substrate and microorganisms, to enhance the SERS sensitivity. The surface modulation with a surfactant could be complimentary towards a variety of microorganisms including hydrophobic microbes, irregular-shaped microorganisms and larger biological cells due to their mutual specific surface interactions. It was anticipated to apply in the rapid detection for varied microbes with label-free and culture-free characterizations.

Received 18th October 2013
Accepted 29th November 2013

DOI: 10.1039/c3tb21469a

www.rsc.org/MaterialsB

Introduction

Nanohybrid arrays of silver (Ag) nanoparticles/nanoscale silicate platelets (NSP) were synthesized from *in situ* reduction of silver nitrate in the presence of the exfoliated silicate clay and demonstrated a high potency in electronics,[1] optical devices,[2] catalysis,[3] fireproof materials and biomedical applications, such as against bacterial growth[4–7] and bio-detection[8–16] *via* surface-enhanced Raman spectroscopy (SERS).

In this study we employed the newly developed nanohybrids consisting of silicate platelet supports and the immobilized Ag nanoparticles for SERS detection evaluation. These silicate nanoplatelets were prepared from the exfoliation of multilayered montmorillonite (MMT) clay with a primary unit structure of lamellar stacks of alumino-silicate platelets, and each platelet of two tetrahedral sheets sandwiches an edge-shared octahedral sheet at 2 : 1 structure at *ca.* 1.0 nm thickness.[17] In the literature, most of the studies[18–23] regarding hybrid materials with Ag nanoparticles are focused on controlling particle sizes, stability and their catalysis properties. The exfoliation of several synthetic and naturally occurring clays including MMT, lucentite SWN and mica to afford NSP nanoplatelets were screened. The NSP from the natural MMT clay with the geometric dimensions of approximately 80 × 80 × 1 nm^3 (ref. 24 and 25) was found to be the most suitable for the bio-detection for SERS due to their high ionic charges on surface, water swelling behavior, and optical transparency and excellent flexibility.

SERS is a recently developed spectroscopic technique based on Raman scattering enhanced by localized surface plasmon resonance (LSPR) and chemical effects.[26–28] The strong Raman signals are from molecules attached to nanometer-sized gold

[a]*Institute of Polymer Science and Engineering, National Taiwan University, Taipei 10617, Taiwan. E-mail: tyliu0322@gmail.com; jianglin@ntu.edu.tw*

[b]*Department of Materials Engineering, Ming Chi University of Technology, New Taipei City 24301, Taiwan*

[c]*Institute of Atomic and Molecular Sciences, Academia Sinica, Taipei 10617, Taiwan*

[d]*Research Program on Nanoscience and Nanotechnology, Academia Sinica, Taipei 11529, Taiwan*

[e]*Institute of Physics, Academia Sinica, Taipei 11529, Taiwan*

[f]*Center for Condensed Matter Sciences, National Taiwan University, Taipei 10617, Taiwan*

[g]*Department of Physics, National Taiwan University, Taipei 10617, Taiwan*

† Electronic supplementary information (ESI) available. See DOI: 10.1039/c3tb21469a

(Au) or silver (Ag) structures. SERS provides the structural information of molecules with high sensitivity and is capable of detecting single molecules non-destructively. Also, this has allowed for extensive chemical and bio-sensing applications including rapid detection of viruses and anthrax,[8,29,30] sensing of specific DNA,[31] and yeast and cell mapping.[32,33] Furthermore, SERS has been employed for label-free sensing of microbes, exploiting its tremendous enhancement in the Raman signal. Recently, a type of SERS-active substrate with uniformly large and highly reproducible Raman-enhancing power has been developed by growing Ag nanoparticles on arrays of anodic aluminum oxide (AAO) nanochannels. Taking the advantage of the sub-10 nm inter-particle gaps in generating 'hot-junctions', an electromagnetic enhancement may be obtained.[13] The high sensitivity and reproducibility of such substrate facilitated the use of SERS for chemical/biological sensing applications.

In order to facilitate SERS for detecting and monitoring of a variety of organisms in environmental and clinical samples, the finding of a flexible SERS could extend the selective detections for irregular-shaped and large organisms such as fungi and cancer cells. The plate-like clay with double-edged sides of anionic surface charges and a large surface area may serve as the suitable supports for anchoring Ag nanoparticles in generating strong hot-junctions [three-dimensional (3D) hot-junctions]. Furthermore, one-to-few nanometer thickness of NSP in association with Ag nanoparticles can offer excellent flexibility and optic transparency, and consequently the close contact between SERS substrate and microorganisms, resulting in the enhancement of SERS sensitivity. The weakness of the conventional SERS in lacking the affinity towards some bacteria with a hydrophobic surface of the cell wall, *ca. E. coli*, and *mycobacteria* could then be overcome. The surface modification by a suitable surfactant, such as polyoxyethylene alkyl ether, ultimately improves the affinity of Ag with bacteria.

Here we report the development of the flexible SERS substrates comprised of silver nanoparticles on nanoscale silicate platelets (Ag/NSP) and optionally modified by a surfactant (Ag/NSS) for advancing the detecting scope of the conventional SERS. Different types of hydrophilic and hydrophobic microorganisms are used to justify the effectiveness of using 3D hot-junctions and flexible nanohybrids.

Results and discussion

Synthesis of the Ag/NSP nanohybrid

The Ag nanohybrids of Ag nanoparticles supported on nanoscale silicate platelets were synthesized by adopting the exfoliated nanoplatelets from the naturally occurred clays of layered structure. In the presence of the silicate nanoplatelets, the reduction of $AgNO_3$ in aqueous medium afforded the nanometer-scale silver particles tethered on the platelet surface. The nanoplatelets with the average dimension of 80–100 nm in width and 1–5 nm in thickness provide the large surface-to-weight ratio for stabilizing the *in situ* generated Ag nanoparticles, as shown in Fig. 1a. The complex of Ag-on-nanoplatelets overcame the inherent aggregation of individual Ag nanoparticles through the platelet surface ionic interaction and van-der Waals attraction. It is particularly noted that Ag nanoparticles are adsorbed on both sides of the NSP surface due to the indiscriminate sandwiching structure of two tetrahedral sheets on an edge-shared octahedral sheet in an individual nanoplatelet. Ag nanoparticles separated by few nanometers-thick of silicate platelet spacers (1–5 nm) could create a huge 'hot-junction' formation and electromagnetic enhancement. Ultimately, it induces strong SERS intensity.

A series of Ag/NSP SERS substrates were prepared by varying Ag/NSP weight ratios from Ag0/NSP100, Ag1/NSP99, Ag7/NSP93, Ag15/NSP85, Ag30/NSP70 to Ag50/NSP50 for evaluating the SERS sensitivity towards bacteria cell walls. The analyses indicated the size of Ag nanoparticles increased from 3.8 nm in Ag1/NSP99 to 35 nm in Ag50/NSP50, corresponding to the trend of increasing Ag composition, as shown in Fig. 1c–g and Table S1.†

3D hot-junctions and flexibility in Ag/NSP SERS substrate

Many theoretical and experimental works[34–38] indicated that the precise control of the gaps in the sub-10 nm regime of the nanostructures is critical for the SERS enhancement. However, it is extremely difficult to prepare such a nanostructure and understand the collective surface plasmons existing inside the gaps. In our previous studies,[13] a SERS-active substrate made of an array of Ag nanoparticles partially embedded in AAO with nanochannels was presented. This substrate exhibits an ultrahigh Raman signal enhancement factor due to the controls of the narrow gaps between the Ag nanoparticles. It represents the first quantitative observation of the collective SERS effect on a substrate with a precisely controlled 'hot junction'[13] by a regime of inter-particle gaps of 5–10 nm in the AAO nanochannels. By comparison, the Ag adsorbed on both sides of NSP provides a new aspect of geometric dimension because of the presence of 3D hot-junctions (x–y–z directions of hot junctions), especially in the z-direction (the gap of inter-particle distance at 1–5 nm thickness of NSP, as shown in Fig. 2a). TEM image (Fig. 2b) shows silver nanoparticles adsorbed on the both sides of NSP. We suggest that the darker particles are Ag nanoparticles on the top side of NSP, whereas grayer ones are on the bottom side (the evidence shows in Fig. S1†). They are separated by exfoliated single layer silicate. Fig. 2c indicates that NSP is in a dimension of approximately $\sim 100 \times 100 \times 1$ nm^3 observed by the cross section TEM image (sample made by the microtome), and also demonstrates that silver nanoparticles adsorbed on both sides of NSP.

Moreover, the few nanometer-thick NSP also displays unique flexible and transparent characteristics. The interaction between Ag/NSP and bacteria was schematically represented and observed by SEM, as shown in Fig. 2d–f. It was expected that the Ag/NSP could adhere onto and entangle around the bacteria surface due to its great flexibility. The result shows that bacteria (*S. aureus*, SA in Fig. 2e and *E. coli*, EC in Fig. 2f) were entangled by thin platelets of Ag/NSP, showing their ultra-flexible or floating behavior, and that the SERS signal could consequently respond (*ca.* 30 seconds) simultaneously by different platelets with less interference effects due to their high transparence. The response could be differentiated or make it easier to contact the irregularly shaped microorganisms through a rapid surface

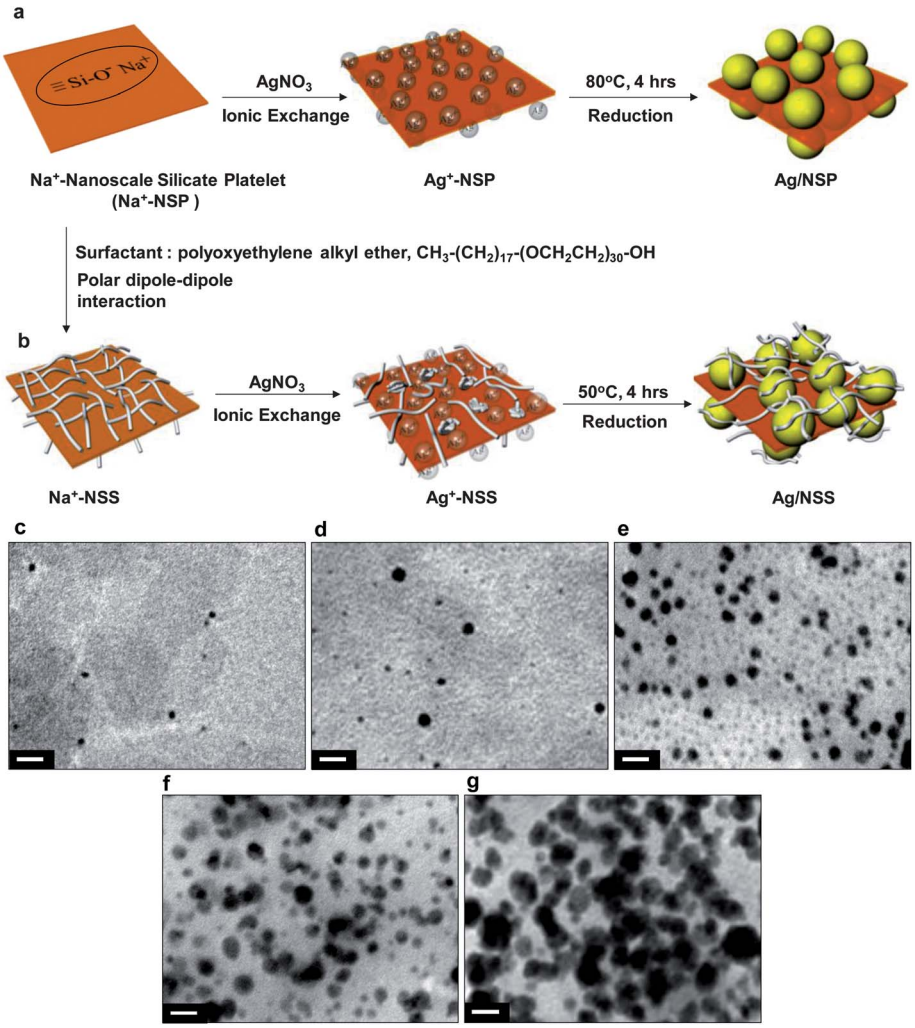

Fig. 1 Schematic illustration of the Ag nanohybrids consisting of Ag nanoparticles on nano-silicate platelets (Ag/NSP). (a) Preparation of Ag/NSP. (b) Preparation of surfactant-modified Ag/NSP (Ag/NSS). (c–g) TEM images of various Ag/NSP weight ratio of compositions: (c) Ag1/NSP99, (d) Ag7/NSP93, (e) Ag15/NSP15, (f) Ag30/NSP70, (g) Ag50/NSP50 (scale bar: 25 nm).

capturing SERS signal without the use of other techniques, such as labeling and culturing.

Relationship between SERS intensity and inter-particle gap

Fig. 3a and Table S1† show the SERS spectra (just the *z*-direction shift) for a different Ag/NSP substrate. The SERS signal of bacteria (SA) displays ~30 times enhancement from Ag1/NSP99 to Ag50/NSP50. The optimal Ag30/NSP70 had a higher reproducibility of SERS intensity owing to the narrow particle size distribution, whereas Ag50/NSP50 had reached the maximum SERS intensity but less reproducibility. Moreover, the displays of low and broad continuous background (*e.g.*, Ag30/NSP70 in Fig. 3a) rendering the improvement of signal interference are compared to the previous development of Ag/AAO array substrate[13] due to their ultra-thin thickness to induce the great optical transparency.

The SERS enhancement appeared to be dependent on the diameter (D) of Ag nanoparticles and their inter-particle gap (W) in the x–y direction, as drawn in Fig. 3b. I_{Stokes} (the average Raman signal per Ag nanoparticle) in the exfoliated single platelet substrate increases in the opposite to the increase of the inter-particle gap. It is explained that the smaller inter-particle gap in this range generates the corresponding larger hot junctions. In reference to the Ag on MMT, the un-exfoliated MMT with 8–10 layered silicate platelets in each multi-layered stack[39] (average thickness: ~20 nm), its I_{Stokes} displays almost half decrease (from 9.3 to 4.3) compared to the similar Ag x–y directional density of the Ag/NSP SERS substrate (Ag15/NSP85, single layer stack) due to same degree of increase in their inter-particle gap in the z-direction (from ~1 nm to ~20 nm) (Fig. 3b and Table S1†). A similar trend was found in the small molecule SERS detection, such as "adenine" from DNA (Table S2† and Fig. 4). The SERS spectra in the bacteria (Fig. 3a) are very similar with adenine (Fig. 4a). We suggest the SERS signal form bacteria might be derived from adenine (DNA) or similar chemical structure compounds released from bacteria.

It is consistent for the factor of the hot junctions in the z-direction. In addition, the hot-junction effect would show up

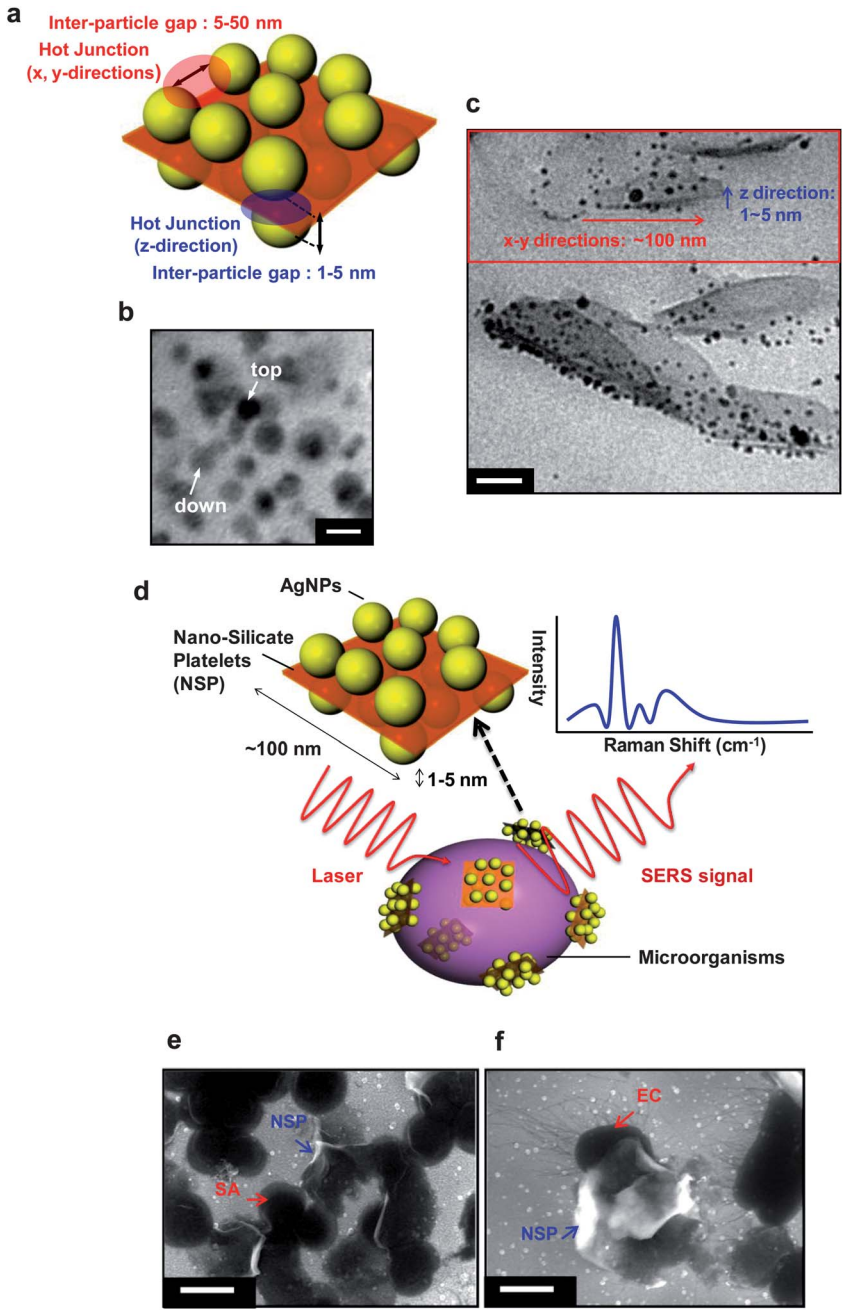

Fig. 2 3-dimensional hot-junctions of Ag/NSP SERS substrate and interaction with bacteria (a) schematic showing 3D hot-junctions (particularly in the *z*-direction) of Ag/NSP SERS substrate; the inter-particle gap in the *z*-direction is about 1–5 nm and in *x*–*y* directions is about 5–50 nm. (b) Top view of the TEM image showing silver nanoparticles adsorbed on both sides of NSP (darker ones: top side; grayer ones: bottom side, scale bar: 20 nm). (c) Cross section of the TEM image showing NSP in a dimension of approximately 100 × 100 × 1 nm^3, and indicating silver nanoparticles adsorbed on both sides of NSP (scale bar: 50 nm). (d) Schematic illustration of Ag/NSP SERS substrate interacting with bacteria, derived from the observations of adhesion and entanglement phenomena taken by the SEM of (e) *S. aureus* (SA) and (f) *E. coli* (EC) interactions (scale bar: 1 μm).

in the change of the absorption spectra (UV-vis spectroscopy), when the *W*/*D* is varied. In principle, there should be at least one absorption peak around 400 nm caused by the plasmon resonance of isolated Ag nanoparticles in water. The existence of a red shift in this plasmon peak is another evidence for the hot-junction effect. The result shows that the smaller the value of *W*/*D*, the wider the red-shifti, as shown in Fig. S2.† In particular, it displays significant red-shift (16 nm wavelength difference) between single-layered platelets (Ag/NSP, inter-particle gap in *z*-direction (W_z): 1–5 nm, 411 nm) and multi-layered silicates (Ag/MMT, W_z: ~20 nm, 395 nm), while showing the corresponding SERS enhancement correlated to the hot-junctions in the *z*-direction (Fig. 5). Such an observation could be then named as the effect of 3D hot-junctions.

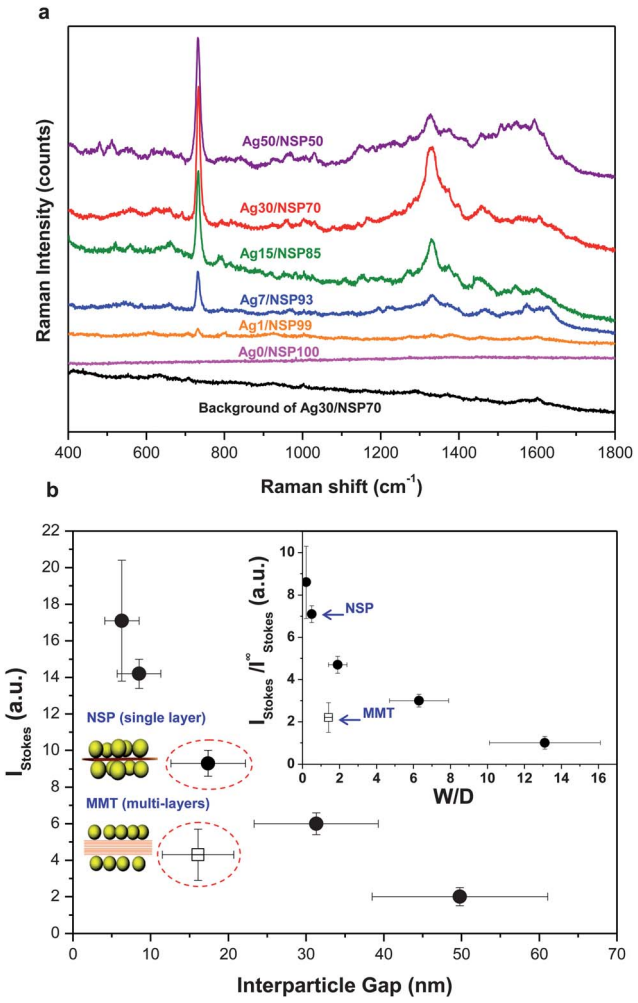

Fig. 3 Relationship between SERS intensity and inter-particle gap of Ag nanoparticles from bacteria. (a) SERS spectra of *S. aureus* (SA) measured by various Ag/NSP weight ratio of SERS substrate. (b) Integrated Raman intensity (I_{Stokes} is the average Raman signal per Ag particle) of SA between 700 and 770 cm^{-1} as a function of the inter-particle gap (W) for different Ag/NSP ratio substrates (un-exfoliated montmorillonite, MMT, thickness: ~20 nm as the reference); the normalized SERS intensity ($I_{Stokes}/I^{\infty}_{Stokes}$ ratio) as a function of the *W*/*D* ratio for different Ag/ASP ratio substrates in the inset figure (I^{∞}_{Stokes} is SERS intensity for the largest inter-particle gap, Ag 1/NSP99, ~50 nm; *D* is the particle diameter measured by TEM).

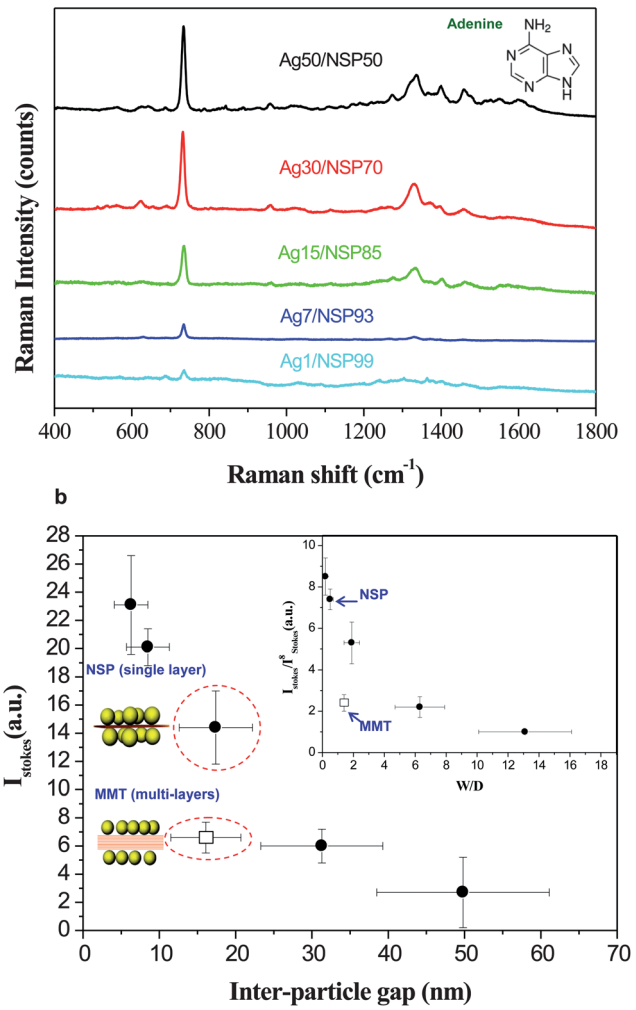

Fig. 4 Relationship between SERS intensity and inter-particle gap of Ag nanoparticles from small molecules. (a) SERS spectra of small molecules (adenine from DNA) measured by various Ag/NSP weight ratio of SERS substrate. (b) Integrated Raman intensity of adenine between 700 and 770 cm^{-1} as a function of the inter-particle gap (*W*) for different Ag/NSP ratio substrates (un-exfoliated MMT as the reference); the normalized SERS intensity ($I_{Stokes}/I^{\infty}_{Stokes}$ ratio) as a function of the *W*/*D* ratio for different Ag/ASP ratio substrates in the inset figure.

The inset in Fig. 3b demonstrated the normalized SERS intensity ($I_{Stokes}/I^{\infty}_{Stokes}$ ratio) as a function of the *W*/*D* ratio for different Ag/NSP substrates. By defining I^{∞}_{Stokes} as the SERS intensity for the highest inter-particle gap of Ag1/NSP99 at ~50 nm, we derived that the ratio of $I_{Stokes}/I^{\infty}_{Stokes}$ of the Ag/NSP SERS substrate (single layer) is much higher than that of the Ag/MMT SERS substrate (multi-layer). For example, the $I_{Stokes}/I^{\infty}_{Stokes}$ ratio equals 4.7 with $W/D = 1.9$ in Ag15/NSP85 in comparison to the ratio at 2.2 in the Ag/MMT SERS substrate with $W/D = 1.4$, indicating about a few times enhancement, as shown in Fig. 3b and Table S1.†

Furthermore, we found that the $I_{Stokes}/I^{\infty}_{Stokes}$ ratio in 3D hot-junctions of Ag/NSP SERS substrate is much higher than that in the traditional 2D hot-junctions of SERS substrates and the literature.[13,34–38] For example, the $I_{Stokes}/I^{\infty}_{Stokes}$ ratio is about 7.1 while *W*/*D* is 0.5 in Ag30/NSP70 (Fig. 3b), whereas the $I_{Stokes}/I^{\infty}_{Stokes}$ ratio is ~1 in 2D hot-junctions of the traditional SERS substrate ($W/D = 0.5$). It shows a 7 times difference of $I_{Stokes}/I^{\infty}_{Stokes}$ ratio between 3D and 2D hot-junctions. From the above observation, it is deduced that a series of Ag/NSP SERS substrates indeed produce enormous electromagnetic effects to induce huge hot-junctions (*x*–*y*–*z* direction hot-junctions) and thus generate the large SERS enhancement. SERS measurement of the small molecule (adenine) exhibits similar conditions with that of the bacteria, as shown in Fig. 4b and Table S2.†

Differentiation of SERS signals between hydrophilic and hydrophobic bacteria

We also found that the intensity of the SERS signal was weaker for detecting hydrophobic bacteria (EC) than for hydrophilic

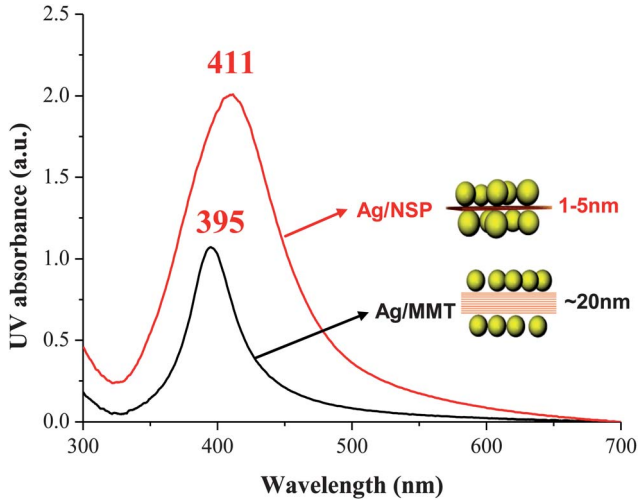

Fig. 5 Relationship between inter-particle gap in z-direction (W_z) and absorption wavelength of Ag/NSP nano-hybrid substrate.

ones (SA), as shown in Fig. 6. Two different bacteria were selected for this investigation. The outer membrane of ECs is comprised of lipo-polysaccharides and proteins as the hydrophobic moieties on the surface, which may mitigate the interaction with Ag/NSP of ionic polarity. With the addition of a surfactant such as the alkyl alcohol ethoxylates (Ag/NSS), they could largely alter the surface affinity of Ag/NSP (conceptually illustrated in Fig. 1a and b and evidenced by the change of Zeta potentials, not shown here). The example of the hydrophobic bacterium (EC) contrasted to the effect of hydrophobic/hydrophilic surface affinity. As a result, the SERS signals (~730 cm^{-1}) of EC/SA ratio changed from 0.07 by Ag/NSP to 0.9 by Ag/NSS, an increase of 13 times in SERS intensity. The SERS enhancement gave rise to the principle of surfactant-modified SERS substrates that differentiated the bacterial species through characteristics and enhancement of the SERS signal intensity.

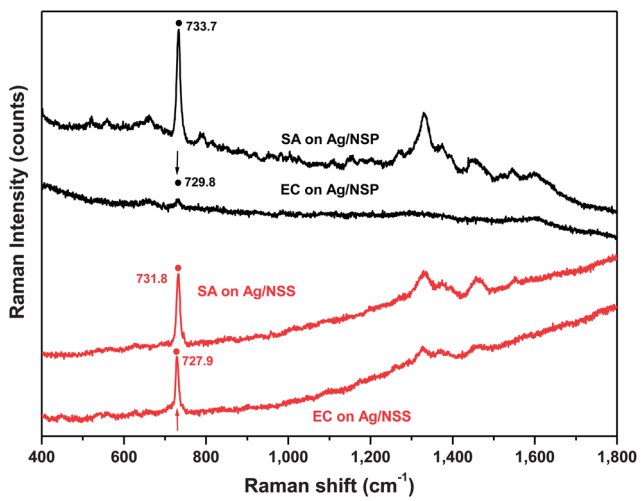

Fig. 6 Differentiation of SERS intensity between Ag/NSP and the surfactant-modified Ag/NSP (Ag/NSS) as SERS substrates for detection of different bacteria. SERS spectra of *S. aureus* (SA, hydrophilic bacteria) and *E. coli* (EC, hydrophobic bacteria) on Ag/NSP *versus* Ag/NSS SERS substrate.

Methods and materials

Synthesis of Ag/NSP SERS substrate

The NSP nanoplatelets (2.0 wt% in de-ionized water) were dispersed by mechanical stirring and added ethanol as the weak reducing agent (Fig. 1a). The NSP dispersion was added with $AgNO_3$ solution (1.0 wt% in water) at the designated ratio of Ag^+ to NSP. The solution was then stirred for another hour. The process involved the replacement of Ag^+ with Na^+ counter ions on the NSP clay surface and, consequently, reducing the Ag^+ by ethanol in a flask. The mixtures were heated to 80 °C for 3 h and monitored by UV-vis spectroscopy for the color change from yellow to deep-red and the completion of Ag^+ reduction to Ag^0.

In the example of Ag/NSP at 7/93 weight ratio, NSP solution (9.36 g, 9.94 wt% in water) were dispersed in deionized water to reach a final concentration of 2 wt%, followed by the addition of ethanol (50 ml). The NSP in the co-solvent of water and ethanol was mechanically stirred for half an hour. Then, $AgNO_3$ (0.11 g) was dissolved in water and added. The Ag/NSP solutions were filtrated and re-dissolved in water to remove the impurities. The preparation of a 2D hot-junction (Ag/MMT) SERS substrate is similar with the 3D hot-junction (Ag/NSP) one. It just replaces NSP by MMT. The UV absorption at ~400 nm of the final solution indicated the formation of Ag nanoparticles. The inter-particle gaps (W) and the particle sizes (D) were measured by a transmission electron microscope (TEM, JOEL JEM-1230) and calculated statistically from an average of at least 100 individual particles with the commercial software (Scanning Probe Image Processor, SPIP™). The stability (UV/vis) tests of Ag30/NSP70 for 4 hours and the heating stability tests at 80 °C for 8 hours were observed in Fig. S3a and S3b,† respectively. These results exhibit strong binding between Ag nanoparticles and NSP, because there is no significant change of UV/vis absorption peak.

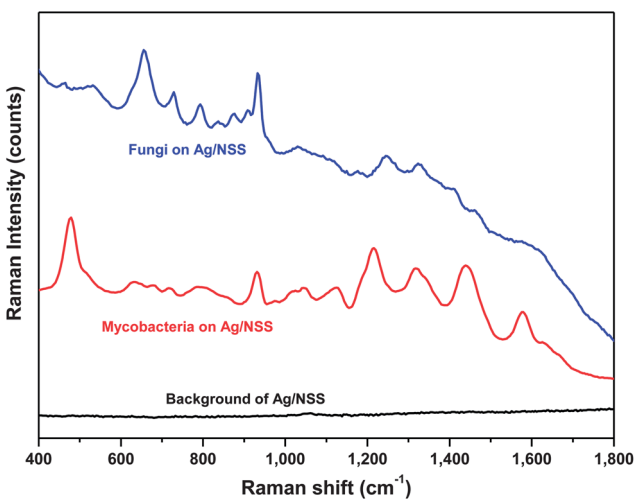

Fig. 7 SERS spectra of mycobacteria (super-hydrophobic bacteria) and fungi (irregular-shaped and larger microorganisms) using Ag/NSS SERS substrate.

Synthesis of Ag/NSS SERS substrate

The procedures for preparing the Ag/NSS nanohybrids are described in the following (Fig. 1b). The NSP dispersion in water was added with SINOPOL 1830 surfactant and abbreviated as NSS. An aliquot of 1 wt% NSP in water suspension (25 g) was added to 1 wt% SINOPOL 1830 in water suspension (25 g) in a round-bottomed flask equipped with a mechanical stirrer for 30 min at room temperature. The NSS solution (50 g, 1 wt% in water) was added with $AgNO_3$ solution (5.9 g, 1 wt% in water) and followed by the procedures mentioned above.

Bacteria growth and sample preparation

Staphylococcus aureus (*S. aureus*, SA) and *Escherichia coli* (*E. coli*, EC) purchased from the Bioresouce Collection and Research Center in Taiwan. Both bacteria were cultivated for 16 h at 37 °C on Nutrient and MRS agar base, respectively. After sub-culturing, single colonies were collected using sterile plastic inoculating loops. Bacteria were then suspended in 5 ml of nutrient and MRS broth, respectively, grown for an additional 14 h and then sub-cultured until OD_{600} reached approximately 0.5. Bacteria thus obtained were used for all the experiments. For SERS detection, bacteria were washed and centrifuged three times with deionized water and re-suspended in water again. Typically, the sample solution (1.0 ml) was placed on a SERS substrate and then stored in an orbital shaking incubator (OSI500R, TKS) operated at 120 rpm and 37 °C for 1 h. The sample was washed five times with water before the Raman performance. The detection limits of bacteria/Ag–NSP ratios should be set in the range of 1 to 30 (one unit of bacteria = 10^8 cfu ml^{-1}; one unit of Ag–NSP = 100 ppm), as shown in Fig. 4.

Characterization

Raman measurements were performed with a commercial Raman microscope (HR800, Horiba). He–Ne laser emitting at 632.8 nm served as the excitation source. The laser beam was focused onto the sample through a 50× objective lens. The backward radiation was collected by the same lens and was then delivered to an 80 cm spectrograph equipped with a liquid-nitrogen cooled charge-coupled device for spectral analysis. Raman spectra were collected in the frequency ranging from 400 to 1800 cm^{-1} with a typical acquisition time of 30 s.

Conclusions

A class of nanohybrids consisting of Ag nanoparticles on both sides of the exfoliated silicate platelets as the support has been developed for the new generation of SERS platform for enhancing the sensitivity of microorganism detection. In contrast to the conventional 2D hot-junctions of traditional "fixed" SERS substrate, the newly developed (3D-hot junctions) SERS substrate provides the enhancement of SERS intensity and detection sensitivity. The observed enhancement is explained by the existence of three dimensional (3D) hot junctions, particularly in the *z*-direction of 1–5 nm inter-particle gap distances, displaying ~7 times increase compared to 2D hot-junctions of traditional "fixed" SERS substrate. The SERS substrate in the exfoliated single silicate platelet (Ag/NSP in 3D hot-junctions) exhibited few times higher than that in un-exfoliated multilayered silicate stack (MMT) in the small molecule (adenine) and bacteria (SA) tests. The SERS spectra fingerprint of adenine corresponds to bacteria. Therefore, we suppose the SERS signal should come from the small molecules released from bacteria.

In addition, the flexible and transparent characteristics (less background interference) of the Ag/NSP SERS substrate could be further modified by the hydrophobic effect of surfactants. It displays about 13 times SERS enhancement in hydrophobic bacteria (*i.e.*, *E. coli*) after being modified by surfactant (Ag/NSS), owing to the affinity increase between SERS substrate and the cell wall of bacteria. The use of 3D hot-junctions of Ag/NSP and surfactant-modified Ag/NSS biochips have broadened the applications for bio-sensing for a variety of microorganisms such as irregular-shaped microorganisms (fungi), super hydrophobic bacteria (mycobacteria) (Fig. 7) and larger biological cells (cancer cells), who are otherwise difficult to be sensitized by 2D hot-junctions of SERS biochips. These findings have advanced SERS technology for the possible creation of SERS-based biochips for rapid label-free and culture-free detection in various microorganisms from clinical patients.

Acknowledgements

This work was financially supported by the National Science Council of Taiwan, the Ministry of Economics of Taiwan, and the Investigator Award of Academia Sinica. We thank Dr Chin-Ching Lin and Dr Hung-Chou Liao from the Industrial Technology Research Institute (ITRI) for suggestions and Yu-An Su for the cross-section of TEM images by the microtome. Technical support from the Core Facilities for Nanoscience and Nanotechnology at Academia Sinica of Taiwan are acknowledged.

References

1 M. Aizawa and J. M. Buriak, *Chem. Mater.*, 2007, **19**, 5090.
2 J. Chen, B. Wiley, J. McLellan, Y. Xiong, Z. Y. Li and Y. Xia, *Nano Lett.*, 2005, **5**, 2058.
3 T. Sun and K. Seff, *Chem. Rev.*, 1994, **94**, 857.
4 S. M. Magaña, P. Quintana, D. H. Aguilar, J. A. Toledo, C. Ángeles-Chávez, M. A. Cortés, L. León, Y. Freile-Pelegrín, T. López and R. M. Torres Sánchez, *J. Mol. Catal. A: Chem.*, 2008, **281**, 192.
5 H. L. Su, C. C. Chou, D. J. Hung, S. H. Lin, I. C. Pao, J. H. Lin, F. L. Huang, R. X. Dong and J. J. Lin, *Biomaterials*, 2009, **30**, 5979.
6 H. L. Su, S. H. Lin, J. C. Wei, I. C. Pao, S. H. Chiao, C. C. Huang, S. Z. Lin and J. J. Lin, *PLoS One*, 2011, **6**, e21125.
7 J. J. Lin, W. C. Lin, R. X. Dong and S. H. Hsu, *Nanotechnology*, 2012, **23**, 065102.
8 R. A. Tripp, R. A. Dluhy and Y. Zhao, *Nano Today*, 2008, **3**, 31.
9 B. D. Moore, L. Stevenson, A. Watt, S. Flitsch, N. J. Turner, C. Cassidy and D. Graham, *Nat. Biotechnol.*, 2004, **22**, 1133.

10 C. M. Shachaf, S. V. Elchuri, A. L. Koh, J. Zhu, L. N. Nguyen, D. J. Mitchell, J. Zhang, K. B. Swartz, L. Sun, S. Chan, R. Sinclair and G. P. Nolan, *PLoS One*, 2009, **4**, e5206.
11 X. Qian, X. H. Peng, D. O. Ansari, Q. Yin-Goen, G. Z. Chen, D. M. Shin, L. Yang, A. N. Young, M. D. Wang and S. Nie, *Nat. Biotechnol.*, 2008, **26**, 83.
12 R. M. Jarvis and R. Goodacre, *Chem. Soc. Rev.*, 2008, **37**, 931.
13 H. H. Wang, C. Y. Liu, S. B. Wu, N. W. Liu, C. Y. Peng, T. H. Chan, C. F. Hsu, J. K. Wang and Y. L. Wang, *Adv. Mater.*, 2006, **18**, 491.
14 T. T. Liu, Y. H. Lin, C. S. Hung, T. J. Liu, Y. Chen, Y. C. Huang, T. H. Tsai, H. H. Wang, D. W. Wang, J. K. Wang, Y. L. Wang and C. H. Lin, *PLoS One*, 2009, **4**, e5470.
15 T. Y. Liu, K. T. Tsai, H. H. Wang, Y. Chen, Y. H. Chen, Y. C. Chao, H. H. Chang, C. H. Lin, J. K. Wang and Y. L. Wang, *Nat. Commun.*, 2011, **2**, 538.
16 T. Y. Liu, Y. Chen, H. H. Wang, Y. L. Huang, Y. C. Chao, K. T. Tsai, W. C. Cheng, C. Y. Chuang, Y. H. Tsai, C. Y. Huang, D. W. Wang, C. H. Lin, J. K. Wang and Y. L. Wang, *J. Nanosci. Nanotechnol.*, 2012, **12**, 5004.
17 R. S. Sinha and M. Okamoto, *Prog. Polym. Sci.*, 2003, **28**, 1539.
18 N. Aihara, K. Torigoe and K. Esumi, *Langmuir*, 1998, **14**, 4945.
19 N. Kakuta, N. Goto, H. Ohkita and T. Mizushima, *J. Phys. Chem. B*, 1999, **103**, 5917.
20 K. Shimizu, S. Komai, T. Kojima, S. Satokawa and A. Satsuma, *J. Phys. Chem. C*, 2007, **111**, 3480.
21 K. Shimizu and A. Satsuma, *Appl. Catal., B*, 2007, **77**, 202.
22 J. Liu, J. B. Lee, D. H. Kim and Y. Kim, *Colloids Surf., A*, 2007, **302**, 276.
23 J. Shibata, K. Shimizu, Y. Takada, A. Shichi, H. Yoshida, S. Satokawa, A. Satsuma and T. Hattori, *J. Catal.*, 2004, **227**, 367.
24 J. J. Lin, C. C. Chu, C. C. Chou and F. S. Shieu, *Adv. Mater.*, 2005, **17**, 301.
25 J. J. Lin, C. C. Chu, M. L. Chiang and W. C. Tsai, *J. Phys. Chem. B*, 2006, **110**, 18115.
26 S. Nie and S. R. Emery, *Science*, 1997, **275**, 1102.
27 Y. Fang, N. H. Seong and D. D. Dlott, *Science*, 2008, **321**, 388.
28 J. Huang, L. Zhang, B. Chen, N. Ji, F. Chen, Y. Zhang and Z. Zhang, *Nanoscale*, 2010, **2**, 2733.
29 X. Zhang, M. A. Young, O. Lyandres and R. P. Van Duyne, *J. Am. Chem. Soc.*, 2005, **127**, 4484.
30 Y. Han, Z. Liang, H. Sun, H. Xiao and H. L. Tsai, *Appl. Phys. A: Mater. Sci. Process.*, 2011, **102**, 415.
31 K. Xu, J. Huang, Z. Ye, Y. Ying and Y. Li, *Sensors*, 2009, **9**, 5534.
32 K. Kneipp, A. S. Haka, H. Kneipp, K. Badizadegan, N. Yoshizawa, C. Boone, K. E. Shafer-Peltier, J. T. Motz, R. R. Dasari and M. S. Feld, *Appl. Spectrosc.*, 2002, **56**, 150.
33 A. Sujith, T. Itoh, H. Abe, K. Yoshida, M. S. Kiran, V. Biju and M. Ishikawa, *Anal. Bioanal. Chem.*, 2009, **394**, 1803.
34 F. J. García-Vidal and J. B. Pendry, *Phys. Rev. Lett.*, 1996, **77**, 1163.
35 L. Gunnarsson, E. J. Bjerneld, H. Xu, S. Petronis, B. Kasemo and M. Kall, *Appl. Phys. Lett.*, 2001, **78**, 802.
36 Y. Lu, G. L. Liu and L. P. Lee, *Nano Lett.*, 2005, **5**, 5.
37 A. Wei, B. Kim, B. Sadtler and S. L. Tripp, *ChemPhysChem*, 2001, **2**, 743.
38 M. Xu and M. J. Dignam, *J. Chem. Phys.*, 1994, **100**, 197.
39 C. C. Chou and J. J. Lin, *Macromolecules*, 2005, **38**, 230.